Water Practice & Technology

IWA PUBLISHING

Water Practice & Technology Vol 16 No 4, 1067 doi: 10.2166/wpt.2021.062

Response of simultaneous nitrification-denitrification to DO increments in continuously aerated biofilm reactors for aquaculture wastewater treatment

Shiyang Zhang[a,*], Jing Chen[a], Julin Yuan[b] and Guangjun Wang[c]
[a] School of Civil Engineering and Architecture, Wuhan University of Technology, Wuhan 430070, China
[b] Agriculture Ministry Key Laboratory of Healthy Freshwater Aquaculture, Key Laboratory of Fish Health and Nutrition of Zhejiang Province, Zhejiang Institute of Freshwater Fisheries, Huzhou 313001, China
[c] Pearl River Fisheries Research Institute, Chinese Academy of Fishery Sciences, Key Laboratory of Recreational Fisheries, Ministry of Agriculture and Rural Areas, Guangzhou 510380, China
*Corresponding author. E-mail: zhangshiyang7@126.com

SZ, 0000-0001-6229-3652

ABSTRACT

Intensive aquaculture usually produces large volumes of nutrient-rich wastewater, which is essential to treat to avoid eutrophication. This study aimed to evaluate the performance of five continuously aerated biofilm reactors treating simulated high-strength aquaculture wastewater under different dissolved oxygen (DO) levels, and the effects of DO increments on simultaneous nitrification-denitrification (SND). Continuous aeration was beneficial to complete nitrification. Total inorganic nitrogen (TIN), principally ammonium, was mainly removed by SND. The SND rate response to different DO levels was fitted well by the power function of $y = 54.81 + 371.58/(1 - 0.16*x)^{(-1/0.24)}$ ($R^2 = 0.897$, $P = 0.000$). When the TIN was removed completely, the optimal SND rate was defined and corresponded to a value of 121.8%. Accordingly, the optimal DO concentration was calculated as 2.10 mg/L, close to the actual level of 1.83 mg/L, at which the highest proportional removals of total nitrogen (58.0%) and TIN (57.3%) were obtained. Phosphorus was also removed by denitrifying polyphosphate-accumulating organisms.

Key words: aquaculture wastewater, biofilm reactor, continuous aeration, dissolved oxygen, percent removal, simultaneous nitrification-denitrification

HIGHLIGHTS

- Dissolved ammonium was mainly removed by simultaneous nitrification-denitrification (SND) process.
- The optimal SND rate for the current wastewater was 121.8%.
- The optimal DO corresponding to the best SND rate was 2.10 mg/L.
- Phosphorus was mainly removed by denitrifying phosphate-accumulating organisms (PAOs).

GRAPHICAL ABSTRACT

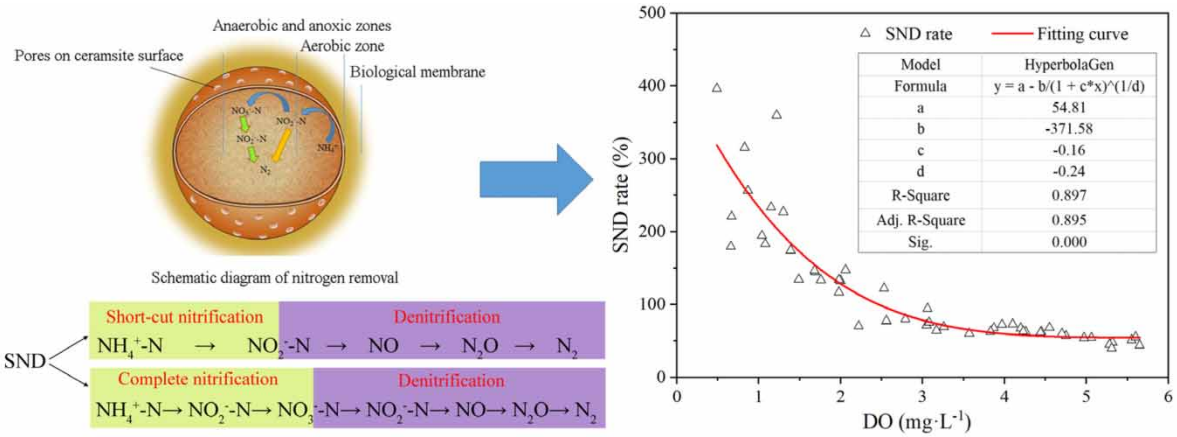

1. INTRODUCTION

With rising living standards, demand for fish protein is increasing. Promoted by the demand for aquatic products, aquaculture expansion, usually involving intensive fish production, is inevitable (Calone *et al.* 2019). Huge amounts of wastewater are still generated during production (Hesni *et al.* 2020). Compared to natural surface waters, intensive aquaculture wastewaters usually contain high concentrations of organics, nitrogen (mainly ammonium), and phosphorus (von Ahnen *et al.* 2018). If discharged directly without proper treatment, such wastewater will cause serious eutrophication. Under increasing pressure for environmental protection, a more effective way to deal with this kind of mixed component wastewater is needed urgently.

Nitrogen removal by the conventional activated sludge process is usually achieved in sequential continuous reactors performing nitrification and denitrification separately (Gao *et al.* 2020). This requires a large area and has the disadvantages of complex operation (Velasco-Garduno *et al.* 2019), poor impact resistance (Li *et al.* 2019), and easy appearance of filamentous bulking (Li *et al.* 2020a). On the contrary, biofilm reactors might be an effective option for intensive aquaculture wastewater treatment (Davidson *et al.* 2019), offering the advantages of convenience, economy, large biomass, strong shock load resistance, and relatively lower sludge yield (Zhang *et al.* 2018; Chai *et al.* 2019). Due to diffusion limitations, anaerobic, anoxic, and aerobic areas may be distributed within the biofilm, forming numerous, similar 'microreactors' under aeration conditions (Cao *et al.* 2017). These might promote simultaneous nitrification-denitrification (SND) in a single reactor, eliminating the need for a separate anoxic compartment (Gao *et al.* 2020) and improving nitrogen removal efficiency (Chai *et al.* 2019). At the same time, due to the role of endogenous denitrification and phosphorus removal, such a reactor has a high carbon utilization rate and can achieve simultaneous nitrogen and phosphorus removal (Wang *et al.* 2015).

Many factors affect the SND rate of biofilm reactors, including the DO concentration, carbon-to-nitrogen (C/N) ratio, packing filler, salinity, etc (Machat *et al.* 2019; Xia *et al.* 2019; Zhang *et al.* 2020a). DO is one of the most critical factors because different DO concentrations affect the number and activity of various functional microbes in the reactor directly. For instance, when DO increases, the number of ammonium-oxidizing bacteria (AOB) and nitrite-oxidizing bacteria (NOB) increases (Cao *et al.* 2017), and the nitrifying and denitrifying capacities increase and decrease respectively (Zhang *et al.* 2020a). DO can also affect the proportions of aerobic and anaerobic areas inside the biofilm directly, and then the microbial community structure (Cao *et al.* 2017; Wang *et al.* 2018), making it one of the most important factors for enhancing the SND rate.

Recently, there have been inconsistent reports on the optimal DO to SND rate. Wang *et al.* (2020) and Cao *et al.* (2017) state that maximum TN/TIN removal was achieved in a moving-bed sequencing batch reactor (SBR) at a DO of 2.5 mg/L when treating synthetic ammonium wastewater. Peng *et al.* (2020) reported that the SND rate in an anaerobic granular SBR reached the maximum of 53.86% at a DO of 2 mg/L. Zhang *et al.* (2020b) reported that the SND rate achieved a maximum of 92.3% in an aerobic biofilm system at a DO of 2 mg/L, when treating real industrial/domestic wastewater. Subtil *et al.* (2019) found that TN removal achieved a maximum of 66% in a single-stage membrane bioreactor at a DO of 0.8 ± 0.1 mg/L. However, there is still little information about the response of SND rate to different DO levels in biofilm reactors for the treatment of high-strength aquaculture wastewater.

In this study a biofilm reactor was used to treat simulated high-strength aquaculture wastewater through SND, to explore the response of SND rate to different DO levels. Using linear fitting between DO and the SND rate, the aim was to determine the optimal level of DO in a biofilm reactor to treat this kind of organic-rich aquaculture wastewater through SND. Ordination analysis between performance and environmental factors was used to obtain the response mechanism of SND to different factors in the biofilm reactor, which would help guide practical application.

2. MATERIALS AND METHODS

2.1. System construction

For this study, five identical SBRs (R1, R2, R3, R4, R5) were constructed of Plexiglas – 20 cm (L and W) × 25 cm (H). They were supported by a 3.5 mm thick PVC plate with a 4.5% perforation rate, above which was 12.5 cm of lightweight, spherical ceramsite (Φ: 3–5 mm; porosity: 0.433). Two aeration sand trays (Φ: 8 cm) were fixed at the bottom of the supporting layer, where a 20 mm drainage hole was drilled. Liquid-level probes were installed near the bottom and top of the reactor, to control liquid volume (Figure 1).

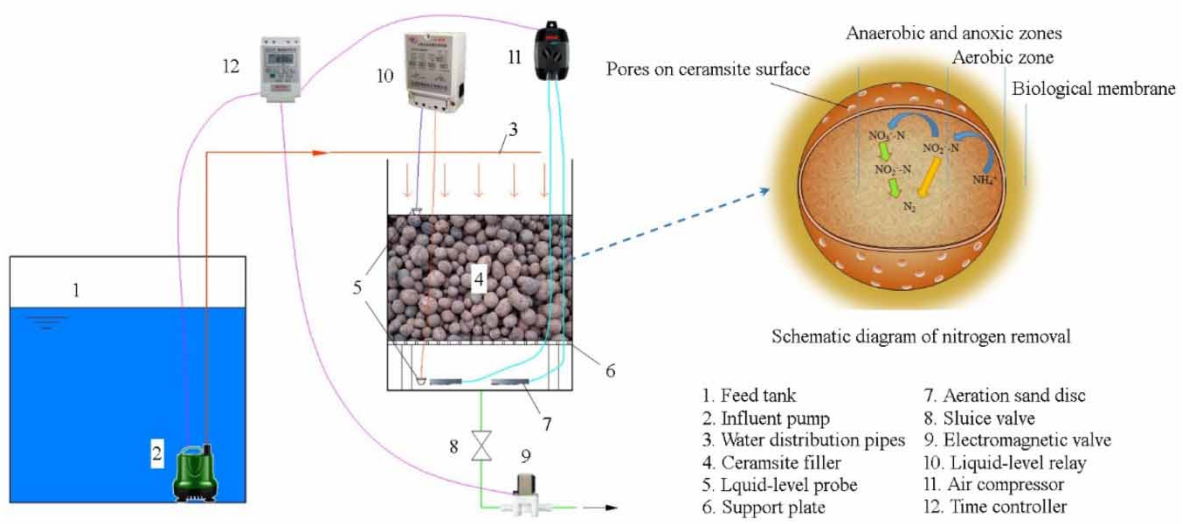

Figure 1 | SBR schematic.

Each SBR had its own, time-controlled aeration system – the two aeration trays in the supporting layer were connected to the same two-chamber micro-air pump (supply rate: 2 × 200 L/h; power: 4 W; maximum lift: 2 m; brand: EHEIM; model: EM3704) through 4 mm internal diameter rubber hoses fitted with check and regulating valves. During feeding, identical influent pumps simultaneously transferred the synthetic high-strength aquaculture wastewater from the same feed tank to the SBRs for subsequent reaction.

2.2. Experimental design

In the study, the SBRs were operated in sequential batch mode with the help of the time controllers and liquid-level relays. The four cycles per day each comprised 3 minutes feeding, 6 hours aeration, and 2 minutes drainage. Unlike conventional SBR operation, no sedimentation or idle stage was set. To explore the impact of DO on reactor performance, the DO levels in R1 to R5 were controlled at around 1, 2, 3, 4, and 5 mg/L (He *et al.* 2009), respectively, by adjusting the valve on the rubber aeration hose.

During start-up, each reactor was inoculated intermittently over 3 days with 3.5 L of activated sludge. The activated sludge came from a previous biofilter operated for simulated high-strength aquaculture wastewater treatment over a year. The reactors' mixed liquid suspended solids (MLSS) concentrations were maintained at approximately 2,000 mg/L. After inoculation, all reactors began treating the aquaculture wastewater for microbial acclimation until maturation, which was characterized by stable carbon, nitrogen, and phosphorus removal in the systems. The hydraulic loading rate (HLR) for the reactors was maintained at 0.35 $m^3/(m^2 \cdot d)$ throughout.

Most pollutants in intensive aquaculture wastewater come from unused feed/excreta (Kokou & Fountoulaki 2018), so the aquaculture wastewater in this study was simulated by dissolving 20 g fish feed (product series: 156, from Tongwei Feed Co., Ltd) in 3 L tap water in a 5 L beaker with magnetic stirring for 5 minutes. After sedimentation for 15 minutes, the supernatant was supplemented with anhydrous sodium acetate (4.90 g), ammonium chloride (2.44), and potassium dihydrogen phosphate (1.09) as carbon, ammonium, and phosphorus sources, respectively, in a 75 L feed tank. The simulated wastewater's final nutrient compositions are shown in Table 1. Trace elements, as described by He *et al.* (2016), were also added to the simulated wastewater and are listed in Table 2.

2.3. Data collection

Daily samples were collected of the raw influent (i.e. the simulated wastewater) and the 6-hour effluents from the reactors. The samples were analyzed for dissolved chemical oxygen demand (DCOD), total chemical oxygen demand (TCOD), nitrite nitrogen (NO_2^--N), nitrate nitrogen (NO_3^--N), total ammoniacal nitrogen (TAN), total nitrogen (TN), inorganic and total phosphorus (IP and TP) using standard methods (APHA 2017). TCOD and TP were determined directly, while DCOD and IP were measured after filtration through a 0.45 μm fiber membrane. Real-time temperature (T), DO, alkalinity (pH), redox potential (ORP), specific conductivity (SC), total

Table 1 | Nutrient composition of the simulated aquaculture wastewater and the corresponding environmental quality limits for surface water in China

Indices	Sources	Concentration in this study (mg/L)	Grade V Standard (mg/L)
DCOD	Fish feed + CH_3COONa	84 ± 13.1	/
TCOD	Fish feed + CH_3COONa	111 ± 12.4	≤40
IP	Fish feed + KH_2PO_4	4.1 ± 0.2	/
TP	Fish feed + KH_2PO_4	4.4 ± 0.2	≤0.4
NO_3^--N	Fish feed	1.9 ± 0.0	/
TAN	Fish feed + NH_4Cl	8.7 ± 0.2	≤2.0
NO_2^--N	Fish feed	0.0 ± 0.0	/
TIN	Fish feed + NH_4Cl	10.6 ± 0.2	/
TN	Fish feed + NH_4Cl	12 ± 0.6	≤2.0
Org-N	Fish feed	1.4 ± 0.5	/
DCOD/TIN		7.9	/

Note: The Grade V Standard is the environmental quality standard for surface water in China (GB3838-2002) (Xu *et al.* 2021).

Table 2 | Trace element content of the simulated wastewater

Item	EDTA	$FeCl_3$	$CaCl_2$	H_3BO_3	KI	$CuSO_4{\cdot}5H_2O$	$MnCl_2{\cdot}4H_2O$	$ZnSO_4{\cdot}7\ H_2O$	$CoCl_2{\cdot}6H_2O$	$Na_2MoO_4{\cdot}2\ H_2O$
Concentration (mg/L)	10.0	0.9	5.0	0.15	0.18	0.03	0.06	0.12	0.15	0.06

dissolved solids (TDS), and salinity (Sal) were measured with a YSI 6600 V2 multiparametric sonde (Yellow Spring Instruments, USA).

2.4. Statistical analysis

Unless stated otherwise, data were expressed as mean ± standard deviation (SD). In this study, total inorganic nitrogen (TIN) was defined as the sum of $TAN + NO_2^- - N + NO_3^- - N$, and, accordingly, organic nitrogen (Org-N) was defined as TN – TIN. Reactor performance in the batch tests was evaluated as proportional removal (%), calculated according to Equation (1):

$$\text{Proportional removal} = (C_{\text{in}} - C_{\text{out}})/C_{\text{in}} \times 100\% \quad (1)$$

where C_{in} and C_{out} indicate influent and effluent pollutant concentrations, respectively. Negative removal indicated accumulation and the accumulation rate was defined as the negative proportional removal (%).

The SND rate was used to evaluate nitrogen removal performance in the reactors, too. Ignoring microbial assimilation and cell death contributions to TAN concentration, the SND rate could be calculated using Equation (2) (Third *et al.* 2003):

$$SND\ rate = \left(1 - \frac{NO_x - N_{produced}}{TAN_{removal}}\right) \times 100\% \quad (2)$$

where NO_x-$N_{produced}$ means the proportion of nitrate/nitrite derived from ammonium oxidation and $TAN_{removal}$ means the total amount of TAN removed. Since the raw influent contained both NO_3^--N and TAN (Table 1), NO_3^--N removal during SND did not all derive from ammonium oxidation. This differed from those cases dealing only with ammonium (He *et al.* 2009; Chai *et al.* 2019; Xia *et al.* 2019; Peng *et al.* 2020). Therefore, the SND rate was only used in this study for impact analysis, without comparison to other cases.

One-way ANOVA (analysis of variance) was used to test the impact of DO level on reactor performance, with LSD (equal variances assumed) or Tamhane's T2 test (equal variance not assumed) for multiple comparisons. Linear fitting between the DO and SND rates was performed to explore the SND rate's response to different

DO levels. Redundancy analysis (RDA) was also employed to evaluate performance and environmental factor relationships. All significance was set at $P < 0.05$.

3. RESULTS AND DISCUSSION

3.1. Comparison of online physicochemical parameters

Table 3 shows that the physicochemical parameters with obvious distinctions between the influent and effluent include *T*, DO, and ORP, while those with limited change include pH, EC, TDS, and salinity. Because the experiment was done in a greenhouse, the wastewater's temperature was significantly below that indoors, so, after a period of retention, the effluent temperature was significantly higher than that of the influent. The significant decrease in effluent DO concentration was attributed to its consumption arising from the oxidation of organics and ammonium (Machat *et al.* 2019). ORP concentration generally reflected those of DO and TAN (Lackner & Horn 2012). The effluent ORP from R1 and R2 was negative – that is, the reactor DO was relatively low and the TAN content relatively high.

There was no significant difference in pH among the effluents, perhaps because of the SND taking place. The alkalinity consumed by nitrification could be supplemented by that produced by denitrification (Wang *et al.* 2020). Nevertheless, the pH of all effluents decreased significantly compared with the influent, for which there are two possible reasons. Firstly, a small amount of sodium acetate was added to the influent as carbon source, which would increase the pH (Li *et al.* 2020b), and its exhaustion – indicated by the low effluent COD concentration, Figure 2(f) – in the reactor, made the effluent pH slightly lower than that of the influent. Secondly, nitrification consumed alkalinity and denitrification produced it, and nitrification in the reactor might be more efficient than denitrification, resulting in a slight decrease in pH (Li *et al.* 2014). This was especially obvious among reactors with high DO levels (Table 3).

3.2. Comparison of treatment performance

As shown in Figure 2, the proportional removal of most pollutants was significantly different among the reactors except for the Org-N index (Figure 2(c)). The latter probably because no stage was set for sludge discharge and suspended sludge was occasionally discharged with the effluent, which was influenced heavily by sampling flow speed. The suspended sludge was composed mainly of organics involving Org-N (Zhang *et al.* 2019).

The effluent nitrite concentrations were all extremely low (no more than 0.05 mg/L) (Figure 2(c)), so the statistical difference in accumulation rate was meaningless. Nevertheless, the lack of obvious nitrite accumulation in the effluent indicated that complete nitrification occurred in the reactors even under the relatively low DO conditions – e.g., in R1 and R2. Several studies show that continuous aeration is helpful to complete nitrification acclimation (Boog *et al.* 2018; Hou *et al.* 2018; Chai *et al.* 2019) even under low DO conditions (Subtil *et al.* 2019), which accords with the present study. Complete nitrification was also demonstrated by the obvious nitrate accumulation at 3 to 5 mg/L DO levels (Figure 2(b)).

With increasing DO, the proportional removal of TAN increased significantly (Figure 2(a)). When the DO concentration was 1 mg/L, almost no TAN was removed. When it was 2 mg/L, the TAN removal rate was below 60%. When it was increased to 3 to 5 mg/L, however, TAN was removed almost completely. Correspondingly, the NO_3-N concentration increased gradually with increasing DO (Figure 2(b)). When DO was 1 to 2 mg/L,

Table 3 | Comparison of online physicochemical parameters between the reactor influents and effluents, with different DO levels

Site	*T* (°C)	DO (mg·L^{-1})	pH	ORP (mV)	EC (μs·cm^{-1})	TDS (g·L^{-1})	Sal (/wt‰)
Influent	11.5 ± 0.8 **a**	11.41 ± 0.32 **a**	7.58 ± 0.25 **a**	206 ± 92 **a**	447 ± 11 **a**	0.29 ± 0.01 **a**	0.22 ± 0.01 **a**
Eff._R1	16.8 ± 0.8 **b**	0.96 ± 0.30 **b**	7.36 ± 0.11 **b**	−46 ± 37 **b**	439 ± 9 **a**	0.29 ± 0.01 **a**	0.21 ± 0.01 **a**
Eff._R2	17.1 ± 0.8 **bc**	1.83 ± 0.39 **c**	7.34 ± 0.12 **b**	−11 ± 27 **bc**	396 ± 59 **ab**	0.26 ± 0.04 **ab**	0.19 ± 0.03 **ab**
Eff._R3	17.7 ± 1.0 **c**	2.93 ± 0.40 **d**	7.33 ± 0.12 **b**	7 ± 24 **c**	368 ± 54 **b**	0.24 ± 0.04 **b**	0.18 ± 0.03 **b**
Eff._R4	17.8 ± 0.9 **c**	4.22 ± 0.29 **e**	7.32 ± 0.12 **b**	18 ± 21 **c**	393 ± 13 **b**	0.26 ± 0.01 **b**	0.19 ± 0.01 **b**
Eff._R5	17.8 ± 0.8 **c**	5.19 ± 0.39 **f**	7.32 ± 0.12 **b**	26 ± 20 **c**	408 ± 6 **b**	0.26 ± 0.00 **b**	0.20 ± 0.00 **b**
P value	**0.000**	**0.000**	**0.001**	**0.000**	**0.000**	**0.000**	**0.000**

Note: Significant differences in columns are marked with different letters.

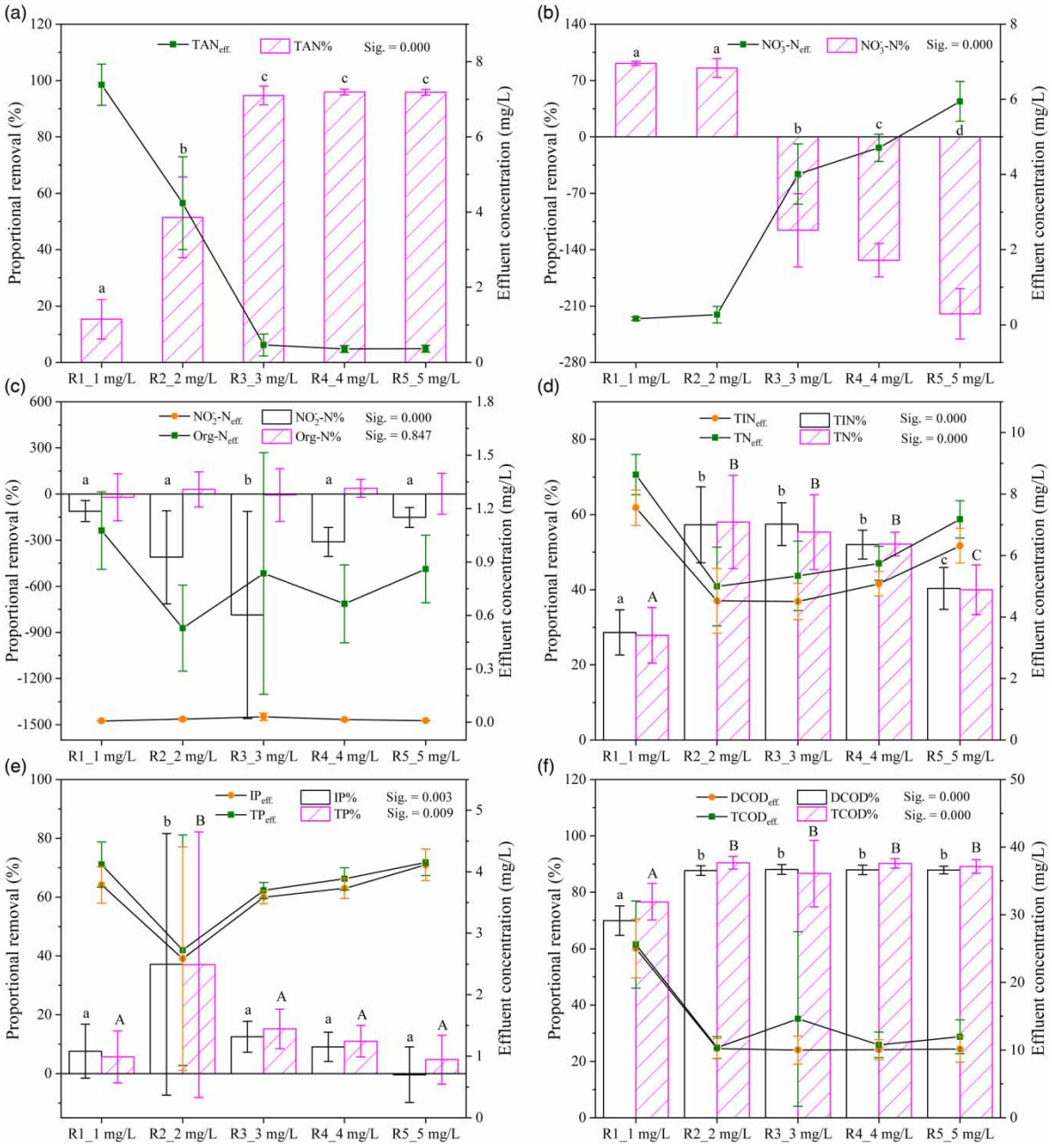

Figure 2 | Comparison of effluent concentration and proportional removals of carbon, nitrogen, and phosphorus in the reactors (a–f). Error bars indicate one SD; lines and columns denote concentration and proportional removal, respectively. Significant differences among columns are marked with different letters.

the NO_3-N removal rate was close to 100%, indicating that both the influent NO_3-N and the proportion of it arising from TAN oxidization were denitrified completely, which also implied that SND was occurring in the reactors.

The TN and TIN concentrations increased significantly at first and then decreased gradually as DO increased from 1 to 5 mg/L (Figure 2(d)). Because the TIN removal denoted the extent of denitrification (Zhang *et al.* 2020a), it was obvious that denitrification efficiency was relatively high when DO was between 1 and 2 mg/L. Since effluent TN was mainly TAN, nitrification was the dominant factor controlling TN removal. Meanwhile, combined with organics removal in R1 and R2 (Figure 2(f)), it could be inferred that increasing the DO concentration to an appropriate level should improve TN removal given the presence of sufficient organics, which could be stored temporarily as an endogenous carbon source (Wang *et al.*

2015). When DO increased from 3 to 5 mg/L, TAN was removed completely and nitrate accumulation increased, while the proportional removal of TN and TIN decreased slowly, indicating that complete nitrification and aerobic denitrification occurred inside these systems. TN and TIN could still be removed when TCOD and DCOD removal was similar and their effluent concentrations were low (Figure 2(f)). This suggested that the reactors could remove nitrogen by endogenous denitrification when the C/N ratio was low (Wang *et al.* 2015), hinting that the carbon source was not the only inhibiting factor for denitrification. It is thought that the decrease of the hypoxic zone due to increased oxygen penetration thickness in the biofilm caused by the increase in DO might be another decisive factor inhibiting denitrification (Cao *et al.* 2017; Wang *et al.* 2018).

In this study, phosphorus displayed a low treatment performance (<40%, Figure 2(e)). Because of the continuous aeration, conditions outside the reactor biofilms were always aerobic (i.e., in the liquid phase – Table 3), perhaps causing constant anoxic/anaerobic conditions inside the biofilm (Cao *et al.* 2017; Wang *et al.* 2018; Jiang *et al.* 2020), thus preventing alternating anaerobic/aerobic conditions over time. This would be detrimental to phosphorus release by conventional PAOs and restrain subsequent phosphorus uptake (Zhao *et al.* 2018). When treating high phosphate concentrations, the packing filler of the ceramsite used in the reactors could easily reach phosphate adsorption saturation (Zhang *et al.* 2019), so the positive phosphorus removal shown in Figure 2(e) arose from microbial assimilation and absorption (Rahimi *et al.* 2011). Moreover, Spearman correlations showed that the TIN/TN removal was positively correlated with that of IP/TP ($R = 0.900$, $P = 0.019$), implying that phosphorus was mainly removed by denitrifying PAOs.

3.3. Response of SND rate to DO variation

From Figure 3(a), it can be seen that each reactor's SND rate decreased with increasing DO. The SND rates in R1 and R2 exceeded 100%, because the influent contained only a small amount of nitrate (Table 1), which resulted in the denitrification rate of nitrate (derived from the influent and ammonium oxidation) exceeding the ammonium nitrification rate. DO was generally the key factor affecting the SND rate (Cao *et al.* 2017). Exploring the relationship between DO and SND rate in the reactor, curve fitting of SND to DO concentration (Figure 3(b)) yielded Equation (3):

$$SND\ rate\ (\%) = 54.82 + \frac{371.59}{(1 - 0.16 * \mathrm{DO})^{\frac{1}{-0.24}}} \tag{3}$$

Since nitrification and denitrification occurred simultaneously, the optimal SND rate was defined on the basis that TIN could be completely removed at the end. When the actual SND rate was below this value, it meant that either the denitrification or the nitrification intensity was weaker – i.e., it could reflect the relative intensity of

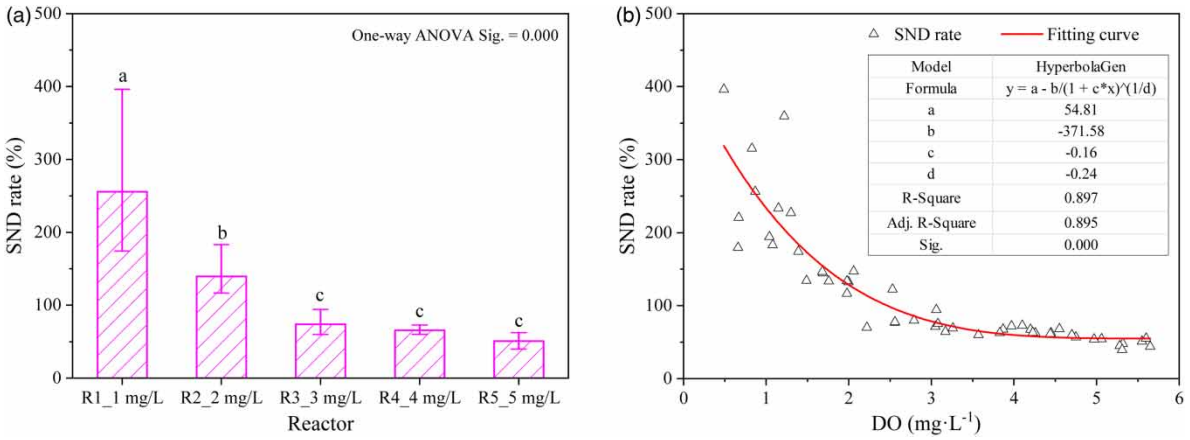

Figure 3 | Comparison of SND rate across the reactors (a) and response to different DO concentrations, with fitting results (b). Significant differences between columns are marked with different letters.

nitrification or denitrification. Following on from Equation (2), the optimal SND rate can be calculated using Equation (4):

$$\text{Optimal } SND \text{ rate} = \left(1 - \frac{-1.9}{8.7}\right) \times 100\% = 121.8\% \quad (4)$$

Taking the optimal SND rate as the expected value, the optimal DO concentration, which would meet the assumption of complete dissolved nitrogen removal, could be calculated. Using the optimal SND rate in Equation (3) gave DO = 2.10 mg/L, which suggested that increasing DO from 1.83 to 2.10 mg/L in R2 could improve TIN and/or TN removal efficiency. This is consistent with the trend shown in Figure 2(d).

3.4. RDA analysis between performance and effluent characteristics

For the on-effluent line parameters (Figure 4(a)), the changes in EC, TDS, and salinity were consistent, and all three were related negatively to the proportional removal of TIN, indicating that NO_x-N removed by denitrification was an important contributor to them. The positive correlation between effluent pH and NO_x-N removal was due to the alkalinity produced by denitrification (Wang *et al.* 2020), while the negative correlation between effluent pH and ammonia removal was due to the alkalinity consumed by nitrification.

The negative correlation between effluent pH and organics removal was attributed to the fact that the sodium acetate is alkaline (Li *et al.* 2020b), its degradation leading to a pH decrease. Meanwhile, the negative correlation between pH and TN/TIN removal might be explained by the large proportion of TAN in the influent, as nitrification, which consumes alkalinity, was the main factor affecting TN/TIN removal.

DO, *T* and ORP correlate negatively with the proportional removal of nitrate, but positively with those of TAN, COD, and TN. These correlations suggest that higher DO concentrations could provide more electron acceptors for heterotrophs and nitrifiers to oxidize organics and TAN, respectively (Machat *et al.* 2019; Jiang *et al.* 2020), and higher temperature could intensify their activity (Ma *et al.* 2020). These conditions would produce more nitrate, facilitating and stronger denitrification processes in the reactors.

For the effluent nutrient indices (Figure 4(b)), proportional TAN removal was positively related to nitrate concentration, because TAN was mainly oxidized to nitrate. TAN removal was also negatively related to effluent TCOD and DCOD because the excess effluent organic content inhibited nitrifier activity (Friedman *et al.* 2018). The obvious positive correlation between TN/TIN removal and nitrite suggested that the ammonium removal path in the reactors might include short-cut nitrification and denitrification (Jiang *et al.* 2020). Proportional TN/TIN removal was negatively correlated with effluent TCOD, DCOD, and TAN, indicating low

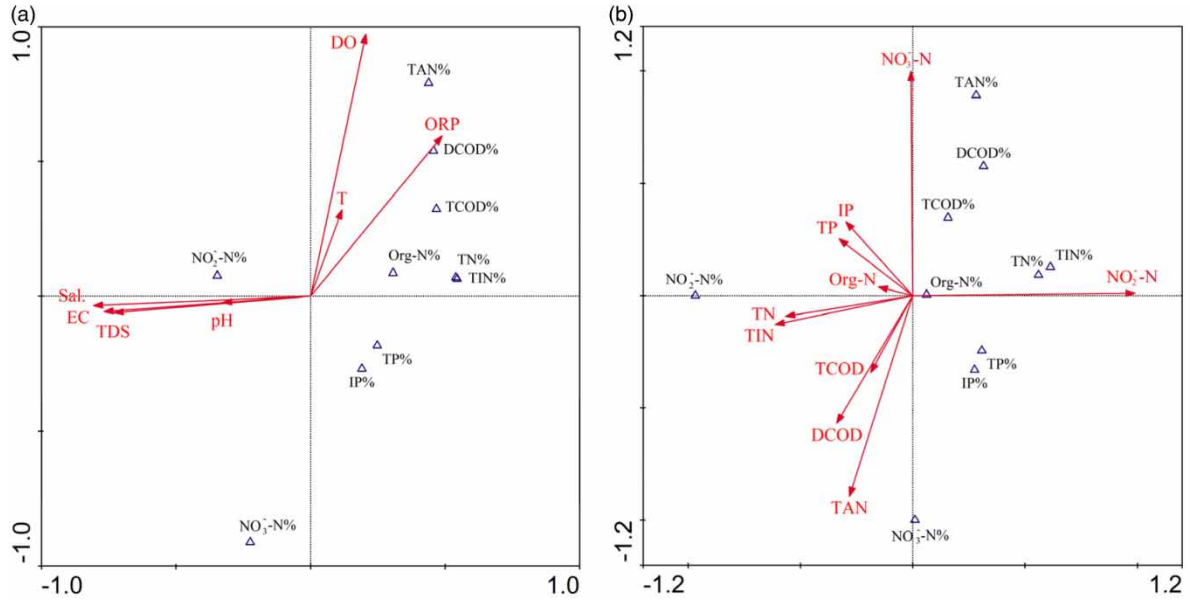

Figure 4 | RDA ordination plots based on treatment performance and effluent characteristics (a) between performance and online parameters and (b) between performance and nutrient indices. Blue triangles denote performance and red arrows the effluent characteristics. The full colour version of this figure is available in the online version of this paper, at http://dx.doi.org/10.2166/wpt.2021.062.

nitrogen removal efficiency when oxidation in the reactor was insufficient. They also implied both insufficient ammonia oxidation capacity (more ammonia remained in the effluent), and insufficient carbon source utilization by denitrification due to the lack of electronic acceptors (not enough nitrate generated). Finally, the proportional removal of TP and IP was significantly negatively correlated with effluent nitrate, TN, and TIN, indicating that denitrifying phosphorus removal was the main path for simultaneous nitrogen and phosphorus removal in the reactors (Wang *et al.* 2015), which was consistent with the previous discussion (section 3.2).

4. CONCLUSIONS

Dissolved nitrogen was largely removed by SND from the aquaculture wastewater. The SND rate's response to different DO concentrations was described by a power function, through which the optimal SND rate or DO concentration could be calculated. Although dissolved nitrogen might be removed completely to meet the stringent environmental quality standard for surface water (GB3838-2002), the reactor displayed a low phosphorus removal performance. The phosphorus was removed mainly by denitrifying PAOs because of the lack of alternating anaerobic/aerobic conditions. Phosphorus could be removed to a greater extent by other processes, however, such as chemical coagulation/precipitation, to meet the environmental standard.

ACKNOWLEDGEMENTS

This work was financially supported by the Key Laboratory of Recreational Fisheries, Ministry of Agriculture and Rural Areas (ZJK201905), the Open Research Program from the Agriculture Ministry Key Laboratory of Healthy Freshwater Aquaculture (ZJK201902), and the Fundamental Research Funds for the Central Universities (WUT: 2019III107CG).

DECLARATION OF INTEREST STATEMENT

The authors declare that they have no known competing financial interests or personal relationships that could have appeared to influence the work reported in this paper.

CREDIT AUTHORSHIP CONTRIBUTION STATEMENT

Shiyang Zhang: Investigation, Data curation & Writing. Jing Chen: Data curation & Analysis. Julin Yuan: Conceptualization, Funding acquisition. Guangjun Wang: Conceptualization, Funding acquisition.

DATA AVAILABILITY STATEMENT

All relevant data are available from the corresponding author.

REFERENCES

APHA 2017 *Standard Methods for the Examination of Water and Wastewater*, 23rd edn. American Public Health Association, American Water Works Association, Water Environment Federation, Washington, DC.

Boog, J., Nivala, J., Aubron, T., Mothes, S., van Afferden, M. & Muller, R. A. 2018 Resilience of carbon and nitrogen removal due to aeration interruption in aerated treatment wetlands. *Science of the Total Environment* **621**, 960–969.

Calone, R., Pennisi, G., Morgenstern, R., Sanye-Mengual, E., Lorleberg, W., Dapprich, P., Winkler, P., Orsini, F. & Gianquinto, G. 2019 Improving water management in European catfish recirculating aquaculture systems through catfish-lettuce aquaponics. *Science of the Total Environment* **687**, 759–767.

Cao, Y. F., Zhang, C. S., Rong, H. W., Zheng, G. L. & Zhao, L. M. 2017 The effect of dissolved oxygen concentration (DO) on oxygen diffusion and bacterial community structure in moving bed sequencing batch reactor (MBSBR). *Water Research* **108**, 86–94.

Chai, H. X., Xiang, Y., Chen, R., Shao, Z. Y., Gu, L., Li, L. & He, Q. 2019 Enhanced simultaneous nitrification and denitrification in treating low carbon-to-nitrogen ratio wastewater: treatment performance and nitrogen removal pathway. *Bioresource Technology* **280**, 51–58.

Davidson, J., Summerfelt, S., Schrader, K. K. & Good, C. 2019 Integrating activated sludge membrane biological reactors with freshwater RAS: preliminary evaluation of water use, water quality, and rainbow trout *Oncorhynchus mykiss* performance. *Aquacultural Engineering* **87**, 12.

Friedman, L., Mamane, H., Avisar, D. & Chandran, K. 2018 The role of influent organic carbon-to-nitrogen (COD/N) ratio in removal rates and shaping microbial ecology in soil aquifer treatment (SAT). *Water Research* **146**, 197–205.

Gao, X. J., Zhang, T., Wang, B., Xu, Z. Z., Zhang, L. & Peng, Y. Z. 2020 Advanced nitrogen removal of low C/N ratio sewage in an anaerobic/aerobic/anoxic process through enhanced post-endogenous denitrification. *Chemosphere* **252**, 7.

He, S.-b., Xue, G. & Wang, B.-z. 2009 Factors affecting simultaneous nitrification and de-nitrification (SND) and its kinetics model in membrane bioreactor. *Journal of Hazardous Materials* **168**(2–3), 704–710.

He, Q. L., Wang, H. Y., Yang, X. J., Zhou, J., Ye, Y. P., Chen, D. & Yang, K. 2016 Culture of denitrifying phosphorus removal granules with different influent wastewater. *Desalination And Water Treatment* **57**(37), 17247–17254.

Hesni, M. A., Hedayati, A., Qadermarzi, A., Pouladi, M., Zangiabadi, S. & Naqshbandi, N. 2020 Using *Chlorella vulgaris* and iron oxide nanoparticles in a designed bioreactor for aquaculture effluents purification. *Aquacultural Engineering* **90**, 102069.

Hou, J., Wang, X., Wang, J., Xia, L., Zhang, Y. Q., Li, D. P. & Ma, X. F. 2018 Pathway governing nitrogen removal in artificially aerated constructed wetlands: impact of aeration mode and influent chemical oxygen demand to nitrogen ratios. *Bioresource Technology* **257**, 137–146.

Jiang, H., Peng, Y. Z., Li, X. Y., Zhang, F. Z., Wang, Z. & Ren, S. 2020 Advanced nitrogen removal from mature landfill leachate via partial nitrification-Anammox biofilm reactor (PNABR) driven by high dissolved oxygen (DO): protection mechanism of aerobic biofilm. *Bioresource Technology* **306**, 11.

Kokou, F. & Fountoulaki, E. 2018 Aquaculture waste production associated with antinutrient presence in common fish feed plant ingredients. *Aquaculture* **495**, 295–310.

Lackner, S. & Horn, H. 2012 Evaluating operation strategies and process stability of a single stage nitritation-anammox SBR by use of the oxidation-reduction potential (ORP). *Bioresource Technology* **107**, 70–77.

Li, H., Zhou, S., Huang, G. & Xu, B. 2014 Achieving stable partial nitritation using endpoint pH control in an SBR treating landfill leachate. *Process Safety and Environmental Protection* **92**(3), 199–205.

Li, M. C., Song, Y., Shen, W., Wang, C., Qi, W. K., Peng, Y. Z. & Li, Y. Y. 2019 The performance of an anaerobic ammonium oxidation upflow anaerobic sludge blanket reactor during natural periodic temperature variations. *Bioresource Technology* **293**, 122039.

Li, W. M., Liao, X. W., Guo, J. S., Zhang, Y. X., Chen, Y. P., Fang, F. & Yan, P. 2020a New insights into filamentous sludge bulking: the potential role of extracellular polymeric substances in sludge bulking in the activated sludge process. *Chemosphere* **248**, 126012.

Li, Y. H., Zhao, J. G., Li, Y., Jin, B. D., Zhang, K. & Zhang, H. Z. 2020b Long-term alkaline conditions inhibit the relative abundances of tetracycline resistance genes in saline 4-chlorophenol wastewater treatment. *Bioresource Technology* **301**, 9, 122792.

Ma, X., Zhao, B. W., Zhang, X., Xie, F., Cui, Y., Li, H. & Yue, X. P. 2020 Effect of periodic temperature shock on nitrogen removal performance and microbial community structure in plug-flow microaerobic sludge blanket. *Chemosphere* **241**, 8, 124934.

Machat, H., Boudokhane, C., Roche, N. & Dhaouadi, H. 2019 Effects of C/N ratio and DO concentration on carbon and nitrogen removals in a hybrid biological reactor. *Biochemical Engineering Journal* **151**, 9, 107313.

Peng, B., Liang, H., Wang, S. & Gao, D. 2020 Effects of DO on N2O emission during biological nitrogen removal using aerobic granular sludge via shortcut simultaneous nitrification and denitrification. *Environmental Technology* **41**(2), 251–259.

Rahimi, Y., Torabian, A., Mehrdadi, N. & Shahmoradi, B. 2011 Simultaneous nitrification-denitrification and phosphorus removal in a fixed bed sequencing batch reactor (FBSBR). *Journal of Hazardous Materials* **185**(2–3), 852–857.

Subtil, E. L., Silva, M. V., Lotto, B. A., Domingues Moretto, M. R. & Mierzwa, J. C. 2019 Pilot-scale investigation on the feasibility of simultaneous nitrification and denitrification (SND) in a continuous flow single-stage membrane bioreactor. *Journal of Water Process Engineering* **32**, 100995.

Third, K. A., Burnett, N. & Cord-Ruwisch, R. 2003 Simultaneous nitrification and denitrification using stored substrate (PHB) as the electron donor in an SBR. *Biotechnology and Bioengineering* **83**(6), 706–720.

Velasco-Garduno, O., Mendoza-Resendiz, A., Fajardo-Ortiz, C. & Beristain-Cardoso, R. 2019 Simultaneous ammonia and organic matter removal from industrial wastewater in a continuous novel hybrid carrousel bioreactor. *International Journal of Environmental Science and Technology* **16**(7), 3429–3436.

von Ahnen, M., Pedersen, P. B. & Dalsgaard, J. 2018 Performance of full-scale woodchip bioreactors treating effluents from commercial RAS. *Aquacultural Engineering* **83**, 130–137.

Wang, X. X., Wang, S. Y., Xue, T. L., Li, B. K., Dai, X. & Peng, Y. Z. 2015 Treating low carbon/nitrogen (C/N) wastewater in simultaneous nitrification-endogenous denitrification and phosphorous removal (SNDPR) systems by strengthening anaerobic intracellular carbon storage. *Water Research* **77**, 191–200.

Wang, J. Y., Rong, H. W. & Zhang, C. S. 2018 Evaluation of the impact of dissolved oxygen concentration on biofilm microbial community in sequencing batch biofilm reactor. *Journal of Bioscience and Bioengineering* **125**(5), 532–542.

Wang, J., Rong, H., Cao, Y. & Zhang, C. 2020 Factors affecting simultaneous nitrification and denitrification (SND) in a moving bed sequencing batch reactor (MBSBR) system as revealed by microbial community structures. *Bioprocess and Biosystems Engineering* **43** (10), 1833–1846.

Xia, Z. G., Wang, Q., She, Z. L., Gao, M. C., Zhao, Y. G., Guo, L. & Jin, C. J. 2019 Nitrogen removal pathway and dynamics of microbial community with the increase of salinity in simultaneous nitrification and denitrification process. *Science of the Total Environment* **697**, 10, 134047.

Xu, S. G., Cui, Y. X., Yang, C. X., Wei, S. J., Dong, W. P., Huang, L. H., Liu, C. Q., Ren, Z. M. & Wang, W. L. 2021 The fuzzy comprehensive evaluation (FCE) and the principal component analysis (PCA) model simulation and its applications in water quality assessment of Nansi Lake Basin, China. *Environmental Engineering Research* **26**(2), 11.

Zhang, J. H., Zhang, L., Miao, Y. Y., Sun, Y. W., Li, X. Y., Zhang, Q. & Peng, Y. Z. 2018 Feasibility of in situ enriching anammox bacteria in a sequencing batch biofilm reactor (SBBR) for enhancing nitrogen removal of real domestic wastewater. *Chemical Engineering Journal* **352**, 847–854.

Zhang, S. Y., Zhu, C. B., Xia, S. B. & Li, M. 2019 Impact of different running conditions on performance of biofilters treating secondary effluent during start-up. *Bioresource Technology* **281**, 168–178.

Zhang, S. Y., Jiang, X. L., Li, M., Zhang, Q., Yuan, J. L. & Guo, W. J. 2020a Effects of deoxygenation pretreatment and dissolved oxygen adjustment on performance of double-layer-packed sequencing biofilm batch reactor treating secondary effluent under low temperature. *Journal of Cleaner Production* **258**, 120650.

Zhang, Y., Zhao, L., Song, T., Cheng, Y., Bao, M. & Li, Y. 2020b Simultaneous nitrification and denitrification in an aerobic biofilm biosystem with loofah sponges as carriers for biodegrading hydrolyzed polyacrylamide-containing wastewater. *Bioprocess and Biosystems Engineering* **43**(3), 529–540.

Zhao, J., Wang, X. X., Li, X. Y., Jia, S. Y. & Peng, Y. Z. 2018 Combining partial nitrification and post endogenous denitrification in an EBPR system for deep-level nutrient removal from low carbon/nitrogen (C/N) domestic wastewater. *Chemosphere* **210**, 19–28.

First received 20 May 2021; accepted in revised form 24 June 2021. Available online 6 July 2021